Available online at www.sciencedirect.com
ScienceDirect
Journal of Colloid and Interface Science 315 (2007) 662–670
JOURNAL OF Colloid and Interface Science
www.elsevier.com/locate/jcis

Friction and adsorption of aqueous polyoxyethylene (Tween) surfactants at hydrophobic surfaces

Malgorzata Graca [a], Jeroen H.H. Bongaerts [b], Jason R. Stokes [b], Steve Granick [a,*]

[a] *Department of Materials Science and Engineering, University of Illinois, Urbana, IL 61801, USA*
[b] *Unilever Corporate Research, Colworth House, Sharnbrook MK44 ILQ, UK*

Received 12 April 2007; accepted 26 June 2007

Available online 13 August 2007

Abstract

The nanotribological responses of a series of nonionic polyoxyethylene surfactants (Tween 20, Tween 40, Tween 60, and Tween 80) were investigated after they were adsorbed from aqueous solution onto atomically smooth hydrophobic substrates. The hydrophobic surfaces were composed of a condensed monolayer of octadecyltriethoxysilane (OTE; contact angle $\theta > 110°$). The nanorheological measurements were performed using a modified surface forces apparatus after coating atomically smooth mica with these OTE monolayers, while adsorption measurements were performed using phase-modulated ellipsometry on silicon wafers coated with these same monolayers. The minimum surface–surface separation observed under high load in friction studies agreed quantitatively with the thickness obtained from ellipsometry. For Tweens 20, 40, and 60, the thickness of the adsorbed film increases with increasing alkyl chain length. Systematic investigations of the nanorheological response showed that there is a "solid-like" elastic response from confined surfactant layers, which is the case for the smallest separations to separations up to slightly larger than twice the adsorbed film thickness. In kinetic friction, these confined layers are characterized by a shear stress of approximately 3 MPa with minimal dependence on shear rate. The magnitude of the sliding shear stress is the same as the apparent yield stress at ≈3 MPa; it is independent of alkyl chain length within the Tween family of surfactants and corresponds to a nominal friction coefficient of $\mu \sim 1$. A similar friction coefficient is observed for boundary lubrication on the macroscopic scale in a tribometer utilizing hydrophobic surfaces and $\mu \approx 1.1$ for Tweens 20, 40, and 60. These results suggest that while Tween molecules adsorb onto hydrophobic surfaces to form a robust separating layer, the lubricating properties of these layers are dominated by a highly dissipative slip plane, the same for all alkyl chain lengths.

Keywords: Tween; Adsorption; Friction; Hydrophobic; SFA; Micelles; Rheology; Tribology; Contact angle; Surfactant; Shear

1. Introduction

Understanding the complexity of surfactant adsorption at solid–liquid interfaces remains one of the main challenges of colloid science. Furthermore, the dynamic properties of surfactants at surfaces on the nanoscale are poorly understood and the literature is relatively sparse, although the subject has been studied for some time [1–3]. These dynamic properties have a large bearing on the (nano)tribological and lubricating properties of surfaces coated by surfactant layers. This is a subject of considerable relevance to many everyday-life systems, such as foods and personal care products, as well as to industrial processes. Most published nanorheological/tribological studies of surfactants have involved ionic surfactants, such as CTAB [4], but we are not aware of a systematic prior study that investigates the tribological properties of nonionic surfactants. In this paper, we aim to fill this knowledge gap by investigating the adsorption of a series of nonionic surfactants (Tweens) onto hydrophobic surfaces as well as the nanotribological/rheological properties of these surfactant-covered surfaces.

No unifying picture has emerged despite extensive studies on the influence of surfactant charge on the kinetics, morphology, structural properties, and mechanisms of adsorption by cationic [5], anionic [6], nonionic [7], and zwitterionic [8] amphiphiles at the liquid–solid interface. These studies show that, depending on the aliphatic chain length, aqueous electrolyte, and surface chemistry of the substrate, surfactants may adsorb

* Corresponding author.
E-mail address: sgranick@uiuc.edu (S. Granick).

0021-9797/$ – see front matter
doi:10.1016/j.jcis.2007.06.057

as hemicylindrical structures, cylindrical aggregates, monolayers, or bilayers.

In this paper, for simplicity we consider the adsorption of nonionic surfactants onto a hydrophobic surface. Previously, it was found [9] that a monolayer forms in this situation, provided that the solid hydrophobic surface is uniform in topography and chemical composition—in other words, is very hydrophobic. As the length of the hydrocarbon chain increases, the hydrophobic interaction between the surfactant and the substrate increases. Moreover, the hydrophobic interaction between neighboring molecules also increases, giving a more closely packed density on the substrate. The amount of longer chain surfactants adsorbed grows more rapidly than in direct proportion to the alkyl chain length [10]. The series of Tweens 20, 40, and 60 varies only in alkyl chain length, which makes this series a good candidate for investigating the influence of alkyl chain length on adsorbed layer thickness.

In the experiments described below, we use the same hydrophobic surface—a condensed monolayer of octadecyltriethoxysilane (OTE) [11–13], formed on a silicon wafer for the contact angle and ellipsometry measurements and on freshly cleaved mica for the friction measurements. From earlier studies [11–13] it is known that extended OTE monolayers are highly hydrophobic (contact angle $>110°$) and show extremely low roughness (root mean square $\sim$3 Å) and the present study confirms this essential premise of the experimental design.

We present contact-angle measurements to establish the quality of hydrophobicity, ellipsometry measurements to determine the adsorbed film thickness, and friction measurements in a modified surface forces apparatus (SFA) to quantify the nanorheological properties of the confined surfactant films. The results of these studies are compared to provide a unifying picture of the adsorption process of a homologous series of polyoxyethylene sorbitans (Tweens). We address the question how monolayers adsorbed onto these hydrophobized surfaces slide past one another in frictional contact. The film thickness and nanorheological results are also discussed in terms of macroscopic tribological measurements in which the same surfactant solutions are used to lubricate compliant hydrophobic surfaces in a tribological setup utilizing macroscopic surfaces that are rough on the molecular scale.

Fragneto et al. [14] quantified how surface coverage grows with solution concentration and went on to show that chains within the adsorbed layer are tilted regardless of surface coverage; the lower the surface coverage, the higher the tilt for all systems that they studied. They concluded that the hydrocarbon chain must lay close to flat on the surface. In contradiction, Cross et al. [15] reported that surfactants with longer alkyl chains form thinner, denser layers when adsorbed to extended hydrophobic surfaces from aqueous solution. This they sought to explain by considering the fluidity of surfactants, which is known to decrease with increasing alkyl chain length [16]. The substrate used in those experiments can be considered as pseudo-hydrophobic, however, as it was prepared through treatment with trimethylchlorosilane. The level of hydrophobicity determined from water contact angle measurements was marginal, with the advancing contact angle of only $71 \pm 2°$.

2. Experimental

2.1. Materials and sample preparation

The following nonionic surfactants, each of them ethoxylated sorbital esters of fatty acids and a polyoxyethylene unit 20 repeat groups long on average, were studied: (a) Tween 20, in which the headgroup is sorbitan monolaurate; (b) Tween 40, in which the headgroup is sorbitan monopalmitate; (c) Tween 60, in which the headgroup is sorbital monostearate; and (d) Tween 80, in which the headgroup is sorbitan monooleate. Tweens 20, 40, and 60 possess 12, 16, and 18 saturated carbons in the alkyl chain, respectively. Tween 80 possess 18 carbons in the alkyl chain and is unsaturated. All of these surfactants are soluble in water with a high value of hydrophilic–lipophilic balance. These surfactants were purchased from Fluka and were used as received. Key properties for the purpose of this study are summarized in Table 1.

For the fabrication of OTE monolayers, *N*-octadecyltrieth-oxysilane was purchased from Hüls America, Inc. In the literature, as different groups have reported variable experiences when it comes to making OTE monolayers of good quality [17–20], it is clear that the resulting monolayers depend highly on details of the experimental protocol. A detailed discussion of the experimental protocols that have been found in this laboratory to be most effective will be presented later (manuscript under preparation). Briefly, previous studies from this laboratory showed that the packing density and degree of crys-

Table 1
A summary of the major physical properties of the Tween surfactants used in this study

	Commercial name			
	Tween 20	Tween 40	Tween 60	Tween 80
Chemical name	Polyoxyethylene (20) sorbitan monolaurate	Polyoxyethylene (20) sorbitan monopalmitate	Polyoxyethylene (20) sorbitan monostearate	Polyoxyethylene (20) sorbitan monooleate
Molecular weight	1228 g/mol	1284 g/mol	1312 g/mol	1310 g/mol
Density (g/ml)	1.105	1.080	1.070	1.064
cmc (mM)	0.059 (0.0072%)	0.027	0.0023	0.012 (0.0016%)
HLB	16.7	15.6	14.9	15.0
Cloud point (°C)	76			65
Viscosity at 25 °C (cP)	330	500	550	425
Phase	Clear liquid	Yellow liquid–gel	Liquid–gel	Golden-yellow viscous liquid

Data are taken from Ref. [30].

tallinity in well-prepared monolayers are comparable to those of a Langmuir–Blodgett film of barium stearate [21]. Furthermore, the thickness of two OTE monolayers in contact in air, measured in a surface forces apparatus, is 51 ± 3 Å relative to mica–mica contact [21]. In order to form monolayers of low roughness, we found it necessary to purify the as-purchased chemical by vacuum distillation at 300 mTorr, at which the liquid was found to boil at 165 °C. Other procedures of OTE monolayer formation were essentially as described earlier by this laboratory [11–13] with the modifications described below. The surface energy of the resulting methyl-terminated surfaces is known to be 22 mJ/m^2 [13].

Tetrahydrofuran (THF), HPLC/spectrophotometric grade, was purchased from Fischer Scientific and used as the solvent for hydrolyzing OTE before monolayer formation. The prehydrolysis solution was a mixture of 0.21 g distilled OTE and 0.125 g 1.3 M HCl, diluted with THF to 25 ml total in a volumetric flask. The solution was held at room temperature for a minimum of 36 h and then diluted with cyclohexane (0.6 g of prehydrolysis solution dissolved in 10 g of cyclohexane) forming the so-called dipping solution. OTE was coated onto silicon wafers (for ellipsometry measurements) and mica sheets (for contact angle and SFA experiments) by immersion in the dipping solution for 35 min. Immediately after removal from the dipping solution the samples were rinsed in a sequence of solvents: cyclohexane followed by 2-propanol and acetone, followed by ultrasonication in each for 3 min to remove the excess nonadsorbed OTE, micelles, or other polymerized clusters from the substrate. In the final monolayer formation step they were baked in a vacuum oven (125 °C) for 2 h. Cyclohexane, 2-propanol, and acetone were purchased from Sigma–Aldrich, HPLC or spectrophotometric grade, and used as received.

To form OTE monolayers on silicon wafers, first the silicon wafers were cleaned in Piranha solution (H_2SO_4:H_2O_2, 7:3) at 75 °C. Silicon cleaned via this method shows hydroxyl (–OH) functional groups, to which OTE can be chemically linked. To form OTE monolayers on mica, first the mica was freshly cleaved manually to produce an atomically smooth and hydrophilic surface of high surface energy. Mica prepared in this way is almost entirely free of –OH functionality, and the silane monolayer is believed to form by the creation of some fraction of Si–O–Si bonds between mica and the OTE monolayer, as described elsewhere [12,13]. It has been shown that this preparation protocol produces a monolayer in which the octadecyl chains are closely packed with crystalline order.

2.2. Contact angle

Contact angles were measured using a home-built setup consisting of a microscope equipped with a goniometer. Droplets of different surfactant solutions were placed at different positions on the test surface. First the advancing contact angle was measured by expelling the droplet through a microsyringe; then the receding contact angle was measured by using the microsyringe to reduce the droplet volume. For each measurement, a new "virgin" part of the hydrophobic surface was used. Contact angle measurements were generally reproducible to within ±0.5°, so long as exactly the same procedure was repeated. Surfactant solutions were prepared using deionized (Nanopure) water.

2.3. Ellipsometry

Ellipsometry, which measures the changes in polarization of light reflected from an interface, was used to infer the in situ thickness of surfactant layers adsorbed from water solution in a specially designed vertical sample cell described in detail by Mukhopadhyay and Law [22]. The vertical configuration allows the hydrophobic sample to be completely submerged in the water. The home-built phase-modulated ellipsometer used for these experiments was modeled after a similar setup described elsewhere [22]. The light source is a very stable 2-mW helium–neon laser ($\lambda = 632.8$ nm). The phase modulator is operated at 50.1 kHz, a photomultiplier tube measures intensity of the reflected light, and the output signal is detected using a lock-in amplifier. Using this setup, in situ thickness of the adsorbed layer is determined with a sensitivity of ∼0.6 Å, subject to the assumption of the appropriate refractive index of the adsorbed layer.

2.4. Surface forces apparatus

The home-built surface forces apparatus in the University of Illinois laboratory, equipped for dynamical viscoelastic measurements in oscillatory shear, has been described previously [23,24]. The geometry consists of two molecularly smooth cylindrical mica surfaces with a curvature radius $R \approx 2$ cm, arranged in crossed cylinder geometry. The surface separation was measured by multiple-beam interferometry and detected by CCD camera using standard techniques with an accuracy of 1–2 Å. In circumstances in which the cylindrical sheets of mica were undeformed by normal forces squeezing them together (relatively large surface–surface separations), the shear forces were normalized by effective contact area by calculating as described in earlier studies from this laboratory [20] the contact diameter with respect to the measured contact diameter at the maximum applied normal force, assuming a Hertzian contact, which is a reasonable assumption when one recalls that it is the glue under the mica that deforms under the action of normal pressure [23]. In the measurements described below, the normal load pressing the sheets of mica together caused the apex of each sheet to deform, producing a locally flattened contact area in which the sheets of mica were parallel to within the experimental uncertainty of thickness measurement. The contact diameter for the thinnest films was calculated from the flattened tip of the interference fringes taking into account the lateral magnification of the focusing mechanism. The shear forces were normalized by the measured contact area to give the shear stress.

The muscovite mica used in the measurements (V-4 grade) was first cleaved and silvered on the backside using standard techniques and then attached to cylindrical quartz lenses using a thermosetting epoxy glue (Norland electronic adhesive). Such prepared lenses were then coated with an OTE monolayer as described above. In the findings described below, surface–surface

separation refers to thickness after subtracting the calibrated thickness of two OTE monolayers in air.

Oscillatory shear deformation was accomplished by mounting the top surface to a small boat rigidly attached to two piezoelectric bimorph strips, for which the dominant motion is bending. The other ends of the bimorphs were fixed in a base support by an epoxy glue. To increase flexibility, each bimorph was lengthened at one end with a short strip of more flexible steel spring by gluing the two. Shear was induced when a voltage difference applied between the two sides of one of the bimorphs bent it. The resulting displacement was transferred to the other bimorph through the rigidly attached boat inducing a voltage difference between the two sides. The comparison of this output voltage when the surfaces are apart, called the calibration output, with that when the surfaces were in contact with the intervening fluid gave information about the response of the fluid to the applied shear. Viscoelastic forces from the confined fluid resist the applied shear motion and result in amplitude attenuation and phase shift in the thin-film situation.

The methods to infer force and motion from voltage induced in piezoelectric bimorphs were described previously [21,23,24]. In brief, the mechanical and the electrical characteristics of the shear device, together with the mechanical behavior of the intervening fluid, were previously modeled and we derived expressions relating the measured amplitude attenuation and the phase shift to the apparent dynamic viscosity and the elastic modulus of the liquid—the mechanical model replaces the device, glue, and liquid with a combination of effective masses, springs, and dashpots. Simply put, a complex impedance, $Z_D = k_D + i\omega b_D$, can be assigned to the device, which responds like an underdamped forced harmonic oscillator when a voltage is applied to the input terminals. Here the real part of the impedance represents the equivalent spring constant of the device, a combination of the spring constants of the bimorphs and the leaf springs. The imaginary part is due to dissipation in the system, mostly caused by the adhesive that holds the bimorphs to the leaf springs. In this configuration the applied stress is split into two, between the device and the combination of glue and liquid. The resulting displacement is the sum of the displacement of the glue and the displacement of the liquid [23]. Earlier studies from this laboratory analyzed the glue displacement in detail and showed that it does not change with time [21,24].

Each experiment began by bringing the OTE-coated mica lenses into contact in air to calibrate the thickness by interferometry and to confirm cleanliness and smoothness of the monolayer surfaces. The surfaces were imaged using standard methods of optical interferometry [25] to give the surface separation and contact (∼45 μm diameter) at the apex of the flattened contact under high normal load. By measuring the oscillatory deflection amplitude and phase in response to an oscillatory shear driving force, effective viscous and elastic shear moduli at the frequency of the drive signal were measured using these piezoelectric techniques [23,24,26].

For subsequent analysis, the shear forces were normalized by contact area to give stress, and stress was normalized to the film thickness to give the effective shear moduli. For this purpose we took the elastic and viscous force constants and normalized by the effective contact area, A_{eff}, and film thickness, D, to give effective shear moduli in and out of phase with the drive, G'_{eff} and G''_{eff}, respectively. Here A_{eff} was estimated by a Hertzian contact as described (see above). Moreover, the dynamic viscosity that quantifies energy dissipation was defined in the traditional rheological way as the loss modulus normalized by oscillatory frequency. Specifically,

$$G'_{\text{eff}}(\omega) = \left[\left(f_{\text{elastic}}(\omega)/d\right)\right][D/A_{\text{eff}}], \tag{1}$$

$$G''_{\text{eff}}(\omega) = \left[\left(f_{\text{viscous}}(\omega)/d\right)\right][D/A_{\text{eff}}], \tag{2}$$

$$\eta'_{\text{eff}}(\omega) \equiv G''_{\text{eff}}(\omega)/\omega, \tag{3}$$

where ω is the radian oscillation frequency and the symbol d refers to the shear amplitude in oscillatory deformation. The elastic force constant is $f_{\text{elastic}}(\omega)/d$ and the viscous force constant is $f_{\text{viscous}}(\omega)/d$. Moreover, it is known that when the amplitude of oscillatory deflection greatly exceeds the film thickness, the viscous response depends not on frequency but on the maximum velocity during the cycle of oscillation, which is the product of frequency and oscillatory shear amplitude [26,27]. Normalizing velocity by film thickness gives the effective shear rate.

Normal loads corresponding to 3 MPa pressure were used to produce the thinnest films, at which the oscillatory shear frequency was swept over the range 1.3 to 287 Hz and displacement amplitude up to 150 nm to produce the range of effective shear rates in the findings described below.

Whereas conventional measurements of linear viscoelastic response concern rheological response that is strictly at the same frequency as the drive frequency, as strains increase, the dynamics of response become nonlinear and higher odd-order harmonics are generated (the even-order harmonics are zero because the stress is an odd function of strain). Detailed considerations described previously [28] show that the energy dissipated over one complete cycle of oscillation is determined by $G''_{\text{eff}}(\omega)$, where this quantity is measured at the drive frequency, i.e., a cancellation of higher order terms signifies that they fail to contribute. With these considerations in mind, in this study we report values of elastic responses only for experiments in which the deformation amplitude was comparable to or smaller than the film thickness.

2.5. Macroscopic tribology

The friction measurements were performed at room temperature ($T = 22 \pm 2\,^{\circ}\text{C}$) on a mini traction machine (MTM; PCS Instruments Ltd., UK). The rubbing contact consists of a poly(dimethylsiloxane) (PDMS) ball with a radius of 0.95 cm and a disk with a radius of 23 mm and a thickness of 4 mm. The root-mean-square roughness of the ball is 26 nm, that of the disk is 9 nm. The Youngs' modulus of the PDMS used is $E = 2.4$ MPa. More details of the preparation of the balls and disks are presented elsewhere [29]. A normal load, L, is applied to the contact by pressing the sphere against the disk and the sphere and disk are rotated at different speeds such that there is a relative motion between the surface of the ball and the disk. This results in a slide-to-roll ratio (SRR), defined as

SRR $= (V_{\text{ball}} - V_{\text{disk}})/U$, where U is the entrainment speed defined as $U = (V_{\text{ball}} + V_{\text{disk}})/2$ and V_{ball} and V_{disk} are the velocities of the ball and disk surface with respect to the contact, respectively. The lateral friction force F_f exerted on the ball is measured through a force transducer, yielding the friction coefficient $\mu = F_f/L$. The applied load is 1 N and the slide-to-roll ratio is set to 50%. Details of the setup and the procedure are reported elsewhere [29,30].

3. Results and discussion

3.1. Contact angle

Atomic force microscopy and ellipsometry have previously suggested that laterally homogeneous layers formed when nonionic surfactants adsorbed to hydrophobic surfaces [7,30,31]. Here we address the influence of the alkyl chain length using Tween surfactants. It is reasonable to expect that Tween surfactants adsorb with the alkyl chain at the hydrophobic surface and the ethylene oxide headgroup, which is water soluble, protruding into the water solution.

Fig. 1 shows advancing (Fig. 1a) and receding (Fig. 1b) angles for Tweens 20, 40, 60, and 80 and also shows how for each of these surfactants the contact angles depend on solution concentration. The contact angle decreases with increasing surfactant concentration. In Fig. 1a, a comparison is made with the critical micelle concentration (cmc) values from the literature and one observes that the advancing contact angle changes abruptly near the cmc and that the facile measurement of contact angle provides a versatile and rapid estimate of the cmc.

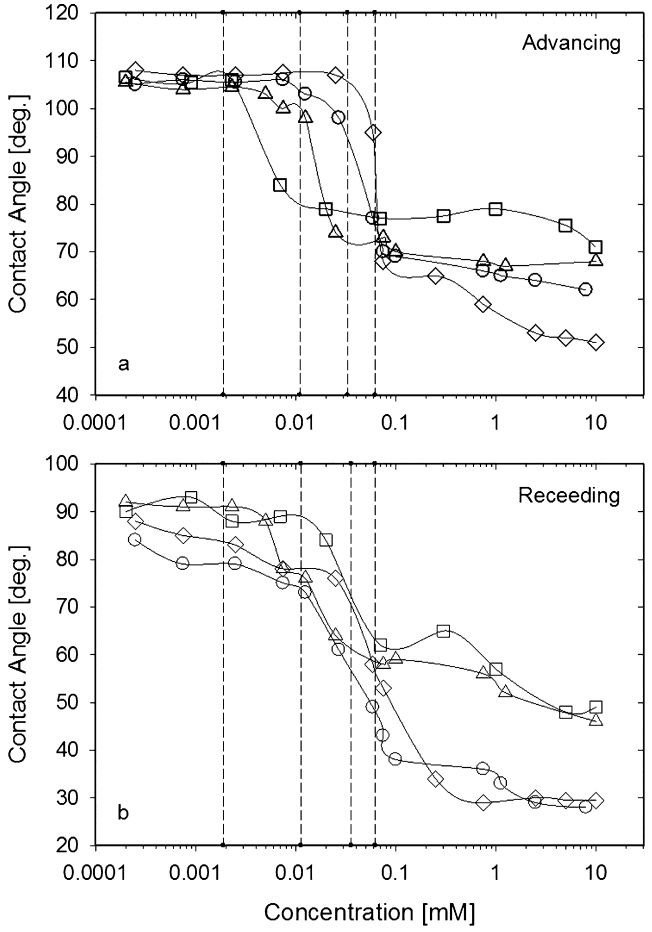

Fig. 1. (a) Advancing contact angle and (b) receding contact angle are plotted against logarithmic solution concentration for the Tween surfactants described in Table 1. Dashed vertical lines indicate literature values of the cmc (critical micelle concentration) of each surfactant. From left to right, the dashed lines refer to the literature cmc [35] of Tween 60 (squares), Tween 80 (triangles), Tween 40 (circles), and Tween 20 (diamonds). Note that the cmc correlates with an abrupt decrease in the advancing contact angle.

3.2. Adsorbed layer thickness

The thickness of the adsorbed surfactant layers, determined from ellipsometry, is shown in Fig. 2. If chains were to stand perpendicular to the surface at close-packed coverage, the thickness would be the end-to-end distance along a molecule, e.g., 5.0 nm in the case of Tween 60. Our measurements consistently showed values less than this—a reasonable finding when one considers that the molecule may stand at an angle $<90°$ and also that an all-*trans* configuration is physically unreasonable in the case of physical adsorption from solution. It is known [14] that the surfactants can tilt at full surface coverage and that the degree of tilt increases systematically with decreasing surface coverage. This leads to a picture in which the alkyl chain must lie close to flat on the surface in cases of dilute-to-moderate surface coverage.

The film thickness values in Fig. 2 were calculated subject to the assumption that refractive index within the adsorbed layers was identical to that of the neat (undiluted) surfactant; deviations from this assumption, allowing a refractive index closer to that of water, would tend to raise the estimated thickness, and indeed the nanorheology experiments presented below suggest this possibility. In Fig. 2, it is striking that the apparent film thickness reaches the expected plateau around the cmc for Tweens 20 and 80 but not for Tweens 60 and 40. In the SFA

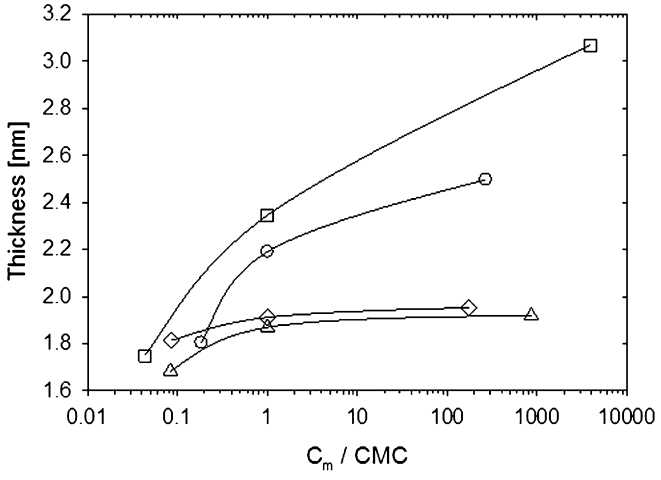

Fig. 2. In situ ellipsometric thickness of the Tween surfactants described in Table 1, each plotted as a function of reduced concentration c/c_{cmc} at ratios from below to above the cmc concentration, under the assumption that the refractive index of the adsorbed layer is identical to that of the bulk surfactant, undiluted by water. Symbols are the same as in Fig. 1.

experiments, the closest surface separation similarly increased with concentration (see below). However, a problematical point, in interpreting this difference, is that each of the samples contained a distribution of headgroup lengths—therefore, the actual surface composition may have changed with concentration in solution, if species of higher molecular weight tended to segregate to the surface in the anomalous cases of Tweens 60 and 40.

However, comparison of relative values in Fig. 2 is not so sensitive to assumptions about the refractive index. In Fig. 2, one observes that the shortest surfactant, Tween 20, formed the thinnest layer. In comparing Tweens 40 and 60, one sees that thickness increased with increasing length of the alkyl moiety. As Tween 80 possesses one unsaturated carbon–carbon double bond in the alkyl moiety, on physical grounds one expects unsaturation to force the molecule to lie more nearly parallel to the hydrophobic substrate. This is probably why, despite the similar extended lengths of the Tween 80 molecule and the Tween 60 molecule, the thickness at full surface coverage was measured to be approximately half that of Tween 60.

We note that these findings appear to contradict the report of Cross et al. [15], who found the opposite, namely that thickness of adsorbed monolayers of the Tween series decreased with increasing length of the alkyl moiety. However, that study employed surfaces considerably less hydrophobic than those used here. In that study, hydrophobicity was produced by treating the surfaces with trimethylchlorosilane, whose single carbon group contrasts sharply with the octadecyl chains of OTE employed in the present study. This may explain why the quoted contact angle of 72° was not characteristic of a highly hydrophobic surface—the contact angle was >30° less than in the present study. The thicker and more hydrophobic alkyl layer used in the present study probably explains why opposite conclusions were obtained here—it is simply because of the lesser tendency of surfactants with long alkyl chains to adsorb to those less hydrophobic surfaces.

Independent confirmation of the ellipsometric thickness determinations came from thickness of the adsorbed Tween layers measured in the surface forces apparatus; here we defined the thickness of one layer as half the separation measured when the surfaces were squeezed together at 3 MPa pressure in the normal direction. The thicknesses of the adsorbed layers for Tween 80, Tween 60, Tween 40, and Tween 20 are 6.70, 6.35, 4.11, and 2.50 nm, respectively. As this slightly exceeds the thickness of 5 nm expected for an extended monolayer of Tween 60, it suggests the possibility of layers slightly thicker than monolayers, which is consistent with the data in Fig. 2. The uncertainty of which refractive index to select for calculations of ellipsometric thickness, noted above, could also contribute to this difference. However, these values of film thickness were measured before, during, and after the samples were sheared and no changes were observed, which indicates that the adsorbed Tween layers remain intact when exposed to the lateral shear stresses in these experiments.

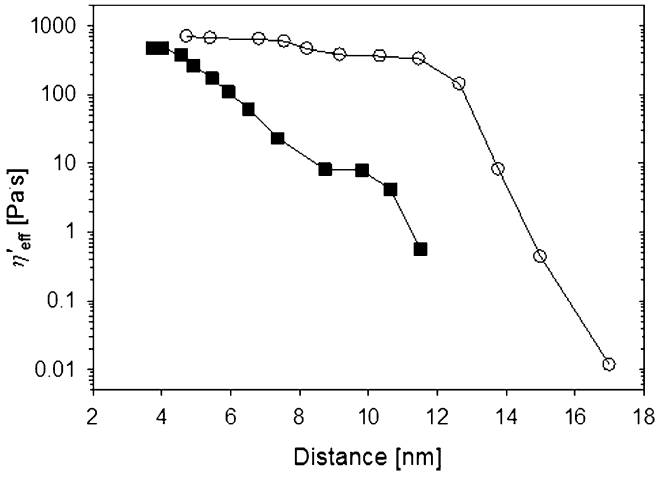

Fig. 3. The logarithmic effective dynamic viscosity of Tween 60/water solution is plotted against film thickness at $c = c_{cmc}$ (0.0023 mM) and at $c = 0.1$ mM, as denoted by squares and circles, respectively. The shear frequency was 97 Hz and the shear amplitude of ≈1 nm corresponded to small strain, where strain is defined as shear amplitude normalized by film thickness.

3.3. Nanorheological and tribological behavior

We now turn to nanorheological measurements of adsorbed Tween layers under confinement. We will discuss first the main features observed for Tween 60; as to the friction behavior, the results for the other Tweens were similar and are left out for brevity.

First, the increase in film thickness with increasing solution concentration was confirmed: the surface–surface separation under high load was 3.7, 4.8, and 6.7 nm at 0.023, 0.1, and 5.5 mM, respectively. Fig. 3 shows for Tween 60 how the logarithmic small-amplitude effective viscosity η'_{eff}, defined by Eq. (3), varied with plate separation. The strain amplitude was kept at a value less than unity. One observes that η'_{eff} exceeds the bulk value for the gaps tested in the surface forces apparatus, indicating the presence of a confined surfactant film. For Tween 60 that is allowed to adsorb from a solution at the critical micelle concentration, η'_{eff} rose by 3 orders of magnitude as the confined surfactant film was squeezed from 12 nm down to 4 nm. Note that the changes appear to be exponential with film thickness, with decay length 2 nm, though no fundamental significance is attached to that at this time.

Other experiments (not shown) led to the conclusion that regardless of the surfactant's concentration in solution during the adsorption process, the effective viscosity for a solution concentration of five times the cmc, η'_{eff}, rose more rapidly at a gap of 14 nm but leveled off to a value of $\eta'_{eff} \approx 10^3$ Pa under compression at the highest loads as the film thickness was decreased, which is only marginally higher than that observed for the solution at the critical micelle concentration.

Findings of this kind were the same regardless of whether the films were squeezed together or pulled apart; no hysteresis was observed. To observe enhanced friction, as indicated by a high effective viscosity, even when the surface separation exceeded twice the film thickness measured by ellipsometry, suggests the presence of some kind of loosely adsorbed layers

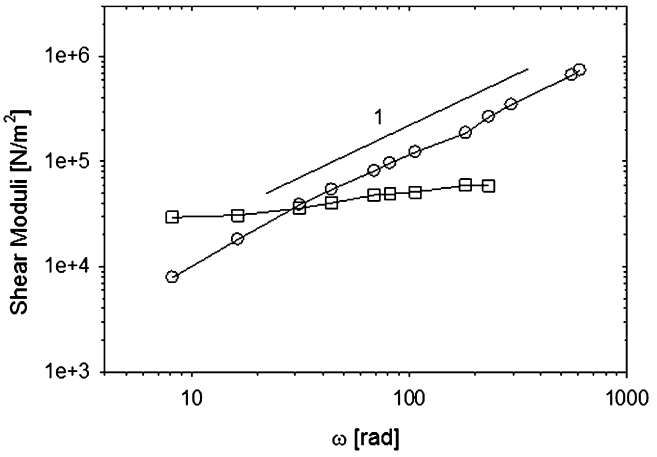

Fig. 4. The elastic and viscous effective shear moduli, $G'_{\text{eff}}(\omega)$ and $G''_{\text{eff}}(\omega)$, are plotted against drive frequency on log–log scales for Tween 20/water solution at $c = 5.5$ mM. Symbols are squares for G'_{eff} and circles for G''_{eff}. The pressure squeezing the surfaces together was 3 MPa and the thickness was 2.5 nm. Data are taken at small strain with shear amplitude ≈1 nm.

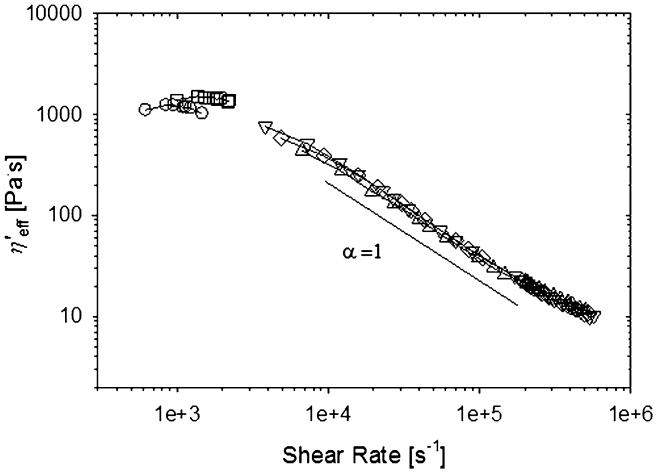

Fig. 5. Effective dynamic viscosity plotted as a function of effective shear rate on log–log scales for a Tween 20/water solution at $c = 5.5$ mM. The shear amplitude is ≈1 nm (open circles), tens of nanometers (squares), <100 nm (triangles), ≈100 nm (diamonds), and ≈150 nm (inverted triangles).

and the necessity of calculating ellipsometric thickness using a refractive index less than that of the neat surfactant. A striking point is the large difference in effective viscosity between 1 and 50 cmc, even at separations less than twice the thickness of an adsorbed layer. This is consistent with Fig. 2 in suggesting that the adsorbed layers restructure significantly as concentration was raised above the cmc.

Fig. 4 shows the frequency-dependent viscous and elastic effective shear moduli, defined by Eqs. (1) and (2), respectively. The example concerns a film of Tween 60 rather than Tween 20 because there appears to be no effect of chain length. The adsorbed layers were compressed by a normal pressure of 3 MPa to a thickness of 6.0 nm. Here again, the amplitude of sinusoidal oscillation is smaller than in other measurements. One observes that the viscous shear modulus grew in linear proportion to frequency. This implies [by Eq. (3)] a constant viscosity and validates the findings plotted in Fig. 3. However, it is intriguing to notice that at the lowest frequencies a marked elastic response exceeded the viscous response. This elastic response increased only weakly with frequency and suggests some kind of paste-like elastic rheological response in this system, even though the viscous response was Newtonian over this range of shear rate.

Next, oscillatory amplitude was raised to larger strains in order to explore the nonlinear responses. Oscillatory amplitudes of up to 150 nm amounted to strain amplitudes of 30 or more and in this regime it is appropriate to consider rheological responses to be functions of effective shear rate rather than oscillatory frequency (similar findings, not shown, were found for each of the other Tween surfactants included in this study). In Fig. 5, the effective viscosity of Tween 20 surfactants allowed to adsorb from a concentration 50 times that of the cmc is plotted on log–log scales against effective shear rate. A regime of constant viscosity (low shear rate) is followed by a regime of shear thinning with power-law decay proportional to shear rate.

Alternatively, the data of Fig. 5 can be represented in terms of viscous shear stress rather than viscosity. In Fig. 6, the viscous shear stress is plotted against effective shear rate on log–log scales for Tweens 20, 40, and 60. One observes an almost constant shear stress of about 3 MPa, the same for all of these surfactants. This can be interpreted as an apparent yield stress of ∼3 MPa and a subsequent constant sliding shear stress at the same value. The small upturn in shear stress with increasing shear rate may be significant but this is as yet unclear. To observe that the three surfactants display the same apparent yield shear stress, despite different surface separation (2.5 nm for Tween 20, 4.1 nm for Tween 40, 6.0 nm for Tween 60), suggests that a slip plane exists, which dominates dissipation upon sliding, and that the slip plane is the same in each of these systems. Hence, the sliding shear stress is not dependent on the length of the alkyl chain.

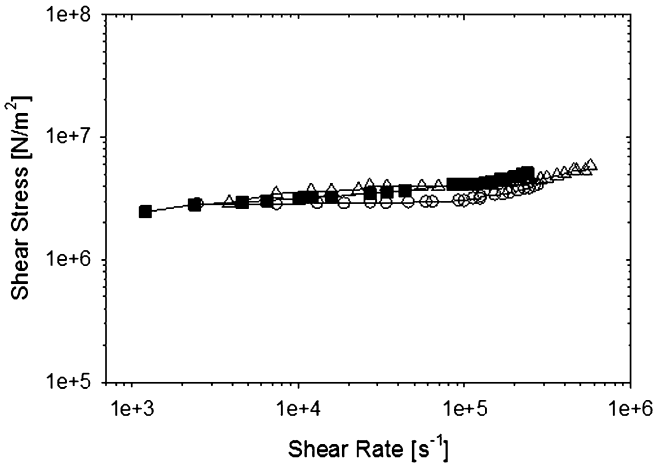

Fig. 6. Same data as in Fig. 5, except that viscous shear stress is plotted against effective shear rate on log–log scales and additional findings are also presented for other Tween surfactants. The data concerning each surfactant are averaged over all data of the kind summarized in Fig. 5 for Tween 20 (circles), Tween 40 (squares), and Tween 60 (triangles). For each surfactant, the measurements are taken at 3 MPa normal pressure: 6.0 nm for Tween 60, 4.1 nm for Tween 40, 2.5 nm for Tween 20. The solution concentration was 5.5 mM.

The limiting sliding shear stress at high shear rate between OTE surfaces in air is four times higher than this, however [32,33]. This shows that in the present situation Tween surfactant layers lower friction below the level that would be characteristic of "dry" sliding of OTE surfaces. The adsorbed Tween layers have the effect of separating the bare OTE layers and lubricating the sliding surfaces. Although the nominal friction coefficient (viscous stress divided by normal pressure) is high, $\mu \approx 1$, we did not observe these systems to degrade with time; they were robust over multiple iterations of the shearing process, at all shear amplitudes and frequencies studied under the current applied load. Along with these robust tribological properties, film thickness also remained constant. This leads to the conclusion that Tween molecules adsorbed on hydrophobic surfaces act as a robust lubricating layer, although this does not result in what are considered to be low friction coefficients ($\mu \ll 1$).

3.4. Comparison of SFA friction values to the macroscopic world

In order to evaluate how results obtained in a "single-asperity" contact in the SFA compare to macroscopic surfaces, we performed parallel tribological experiments using a contact that consists of a sphere with a diameter of 0.925 mm, sliding and rolling against a flat disk. The sphere and disk were made out of PDMS and were hydrophobic, with a contact angle for water of $\theta \approx 100°$, similar to the value for the OTE layers used in the SFA experiments. The substrates were compliant and, at a load of 1 N, gave a contact diameter of 2.4 mm and an average pressure of 0.22 MPa, 1 order of magnitude less than in the SFA experiments. The second major difference compared to the SFA experiments is that the surfaces are not smooth on the atomic scale. The root-mean-square roughnesses of the ball and disk were 25 and 9 nm, respectively.

Fig. 7 shows the friction coefficients in the case in which water lubricates the contact as well as for Tween solutions at a concentration of 5.5 mM, the same concentration as for the SFA experiments in which the friction coefficients were determined. The horizontal plateau observed for water at low speeds is the so-called *boundary lubrication* regime, where the rubbing surfaces are in direct contact. For water in between PDMS surfaces, the friction coefficient in this regime is identical to that of a dry contact, because water is squeezed out from the contact. At higher speeds, the friction decreases into the *mixed-lubrication* regime, due to hydrodynamic lift being able to reduce the number of asperity contacts.

In the case in which Tween solutions were used as the lubricant, the mixed regime shifted to lower speeds. We attribute this to enhanced fluid entrainment into the contact, facilitated by the adsorption of a monolayer of surfactant on the hydrophobic surfaces, effectively rendering them hydrophilic (manuscript in preparation).

As the SFA inherently measures boundary lubrication, we compare the effective friction coefficients obtained from the SFA measurements ($\mu^{\mathrm{SFA}}_{\mathrm{Tween}} \approx 1$) to those obtained at the lowest possible speed in the macroscopic measurement, $U = 1$ mm/s.

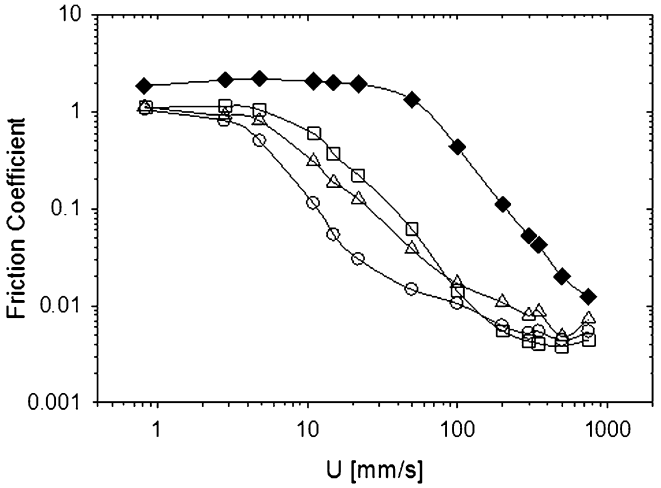

Fig. 7. Macroscopic friction coefficients, measured on standard tribology equipment, as a function of entrainment speed U for the case of water and Tween solutions (Tweens 20, 40, and 60) used as the lubricant. The surfactant concentration is 5.5 mM in all cases. Symbols denote Tween 20 (circles), Tween 60 (triangles), Tween 40 (squares), and water (diamonds).

Fig. 7 shows that the boundary friction coefficient at $U = 1$ mm/s was reduced from a value of $\mu^{\mathrm{MTM}}_{\mathrm{water}} \approx 2$ for water to a value of $\mu^{\mathrm{MTM}}_{\mathrm{Tween}} \approx 1$ and that this value was, within experimental accuracy, identical for all Tween solutions (20, 40, and 60). This reduction for the Tween solutions is significant compared to water, but the value for μ is still considered to be high. Considering the fact that the pressures within the rubbing contacts as well as the surface roughness are quite different for the two setups, the qualitative and quantitative agreement between the measurements using the SFA and those obtained using macroscopic rough surfaces is striking. These results demonstrate that SFA measurements on the nanoscale can be translated to the macroscopic world.

Parenthetically, we note that while Tween 80 results were discussed in terms of the adsorption measurements, we have left them out of the comparison for the nanotribology experiments because the adsorption experiments already pointed to an insignificant effect. It is interesting to note that the friction coefficients measured in both nanotribology and macrotribology experiments presented in this paper are larger than observed by Rutland and coworkers in a study based on using atomic force microscopy and a cellulose bead [34], perhaps because the surfaces in that study were less hydrophobic.

4. Conclusions

The nanotribological response of a series of nonionic polyoxyethylene surfactants (Tween 20, Tween 40, Tween 60, and Tween 80) has been investigated after adsorption from aqueous solution onto condensed monolayers of OTE (contact angle $\theta > 110°$). The minimum surface–surface separation observed in friction studies agreed quantitatively with the thickness obtained from ellipsometry. For Tweens 20, 40, and 60, the thickness of the adsorbed film increased with increasing alkyl chain length. Systematic investigations of the nanorheological response showed that there is a "solid-like" elastic response from

confined surfactant layers, which is the case for the smallest separations to separations up to slightly larger than twice the adsorbed film thickness. In kinetic friction, these confined layers are characterized by a shear stress of approximately 3 MPa with minimal dependence on shear rate. The magnitude of the sliding shear stress was the same as the apparent yield stress at ≈3 MPa; it was independent of the alkyl chain length within the Tween family of surfactants and corresponded to a nominal friction coefficient of $\mu \sim 1$. A similar friction coefficient was observed for boundary lubrication on the macroscopic scale in a tribometer utilizing hydrophobic surfaces and $\mu \approx 1.1$ for Tweens 20, 40, and 60. These results suggest that while Tween molecules adsorb onto hydrophobic surfaces to form a robust separating layer, the lubricating properties of these layers are dominated by a highly dissipative slip plane that is identical for all alkyl chain lengths.

Acknowledgments

This work was supported by a grant from Unilever Corporate Research (UK), using facilities supported by a grant to the University of Illinois from the National Science Foundation, NSF-CMS-05-55820. Partial equipment support was also provided by NSF-DMR-0071761, the NSF Nanoscience Engineering Initiative, and the Science and Technology Center for Purification of Water, NSF CTS-0120978.

References

[1] F.P. Bowden, D.D. Tabor, The Friction and Lubrication of Solids, vols. I and II, Oxford Univ. Press, Oxford, 1964.
[2] B.J. Briscoe, D.C.B. Evans, Proc. R. Soc. London A 380 (1982) 389.
[3] H. Suda, Langmuir 17 (2001) 6045, and references therein.
[4] S. Perkin, N. Kampf, J. Klein, J. Phys. Chem. B 109 (2005) 3832.
[5] S. Manne, J.P. Cleveland, H.E. Gaub, G.D. Stucky, P.K. Hansma, Langmuir 10 (1994) 44009.
[6] R. Lamont, W.A. Ducker, J. Colloid Interface Sci. 191 (1997) 303.
[7] H.N. Patrick, G.G. Warr, S. Manne, I.A. Aksay, Langmuir 13 (1997) 4349.
[8] L.M. Grant, W.A. Ducker, J. Chem. Phys. B 101 (1997) 5337.
[9] L.M. Grant, T. Ederth, F. Tiberg, Langmuir 16 (2000) 2285.
[10] T.P. Goloub, L.K. Koopal, Langmuir 13 (1997) 673.
[11] G. Carson, S. Granick, J. Appl. Polym. Sci. 37 (1989) 2767.
[12] C.R. Kessel, S. Granick, Langmuir 7 (1991) 532.
[13] J. Peanasky, H.M. Schneider, S. Granick, C.R. Kessel, Langmuir 11 (1995) 953.
[14] G. Fragneto, J.R. Lu, D.C. McDermott, R.K. Thomas, A.R. Rennie, P.D. Gallagher, S.K. Satija, Langmuir 12 (1996) 477.
[15] G.H. Cross, A. Reeves, S. Brand, M.J. Swann, L.L. Peel, N.J. Freeman, J.R. Lu, J. Phys. D Appl. Phys. 37 (2004) 74.
[16] A. Mukhopadhyay, B.M. Law, Phys. Rev. E 62 (2000) 5201.
[17] Y. Liu, K. Wolf, M.C. Messmer, Langmuir 17 (2001) 4329.
[18] A.Y. Fadeev, T.J. McCarthy, Langmuir 16 (2000) 7268.
[19] T. Vallant, J. Kattner, H. Brunner, U. Mayer, H. Hoffman, Langmuir 15 (1999) 5339.
[20] A. Ulman, Chem. Rev. 96 (1996) 1553.
[21] H.-W. Hu, S. Granick, Langmuir 10 (1994) 3857.
[22] A. Mukhopadhyay, Ellipsometric Study of Surface Phenomena, Ph.D. thesis, Kansas State Univ., Manhattan, 2000.
[23] A.L. Demirel, S. Granick, J. Chem. Phys. 115 (2001) 1498.
[24] J. Peachey, J. Van Alsen, S. Granick, Rev. Sci. Instrum. 62 (1991) 463.
[25] J.N. Israelachvili, J. Colloid Interface Sci. 44 (1973) 259.
[26] S. Granick, Science 253 (1991) 1374.
[27] H.-W. Hu, G. Carson, S. Granick, Phys. Rev. Lett. 66 (1991) 2758.
[28] S. Granick, H.-W. Hu, G.A. Carson, Langmuir 10 (1994) 3874.
[29] J.H.H. Bongaerts, J.R. Stokes, K. Fourtouni, Tribol. Int. (2007), doi:10.1016/j.triboint.2007.01.027.
[30] J. de Vicente, J.R. Stokes, H.A. Spikes, Tribol. Lett. 20 (2005) 273.
[31] S.B. Velegol, B.D. Fleming, S. Biggs, E.J. Wanless, R.D. Tilton, Langmuir 16 (2000) 2548.
[32] G. Reiter, A.L. Demirel, S. Granick, Science 263 (1994) 1741.
[33] G. Reiter, A.L. Demirel, J. Peanasky, L. Cai, S. Granick, J. Chem. Phys. 101 (1994) 2606.
[34] K. Theander, R.J. Pugh, M.W. Rutland, J. Colloid Interface Sci. 291 (2005) 361.
[35] A. McPherson, Crystallization of Biological Molecules, Cold Spring Harbor Laboratory Press, New York, 1999.